Physica C 152 (1988) 161–170
North-Holland, Amsterdam

STRUCTURE AND FORMATION OF TWINS IN THE ORTHORHOMBIC $YBa_2Cu_3O_{7-x}$

Mehmet SARIKAYA, Ryoichi KIKUCHI and Ilhan A. AKSAY
Department of Materials Science and Engineering, and Advanced Materials Technology Program, Washington Technology Center, University of Washington, Seattle, WA 98195, USA

Received 19 January 1988

Structure and formation of twins in the orthorhombic phase of $YBa_2Cu_3O_{7-x}$ samples, exhibiting bulk superconductivity at 90 K, are studied by transmission electron microscopy and modeling. Twinned domains with {110} twin boundaries form with separation λ which is dictated by energetic and geometrical requirements. Both of these requirements are related to $\Delta a = b - a$, where b and a are lattice parameters of the orthorhombic phase. Geometrical requirement leads to the estimate that the stable values of λ are integer multiples of $d = ab/(\sqrt{2}\Delta a)$. In some samples λ's are regular, in others not. Deviation of λ from theoretically expected stable separations is interpreted as due to local variation of oxygen ordering and/or local elastic strain. The twin boundary has a structure different from the bulk orthorhombic phase and electron micrographs suggest that it has a width of 30–50 Å. In bulk samples twinned domains can be present at different stages of the growth process. These substructural variations suggest that samples are at metastable equilibrium and are consistent with samples being in the superconducting glassy state.

1. Introduction

Recently, there is a growing interest in the possible effects of substructural variations, i.e., various lattice defects and inhomogeneities at nanometer range, to the superconducting properties of $YBa_2Cu_3O_{7-x}$ phase. For example, some latest measurements perfomed on high-T_c oxides on susceptibility and magnetization [1] and microwave absorption [2] have been interpreted to be due to these compounds being in a superconducting glassy state, as discussed by Deutscher and Müller [3]. Furthermore, it was suggested that single-crystal critical current measurements [3] are consistent with the disappearance of the glassy behavior, which may be caused by twins, at low temperatures [4]. In relation to twin formation in these compounds, it was found that there are local structural variations and that $\Delta a/a$, where $\Delta a = b - a$ (b and a being the lattice parameters of the orthorhombic phase) varies between zero and 4.0%, while the values measured from the bulk samples for a (3.826 Å) and b (3.891 Å) correspond to $\Delta a/a$ equal to 1.8%. The variation in $\Delta a/a$ was attributed to variations in the local oxygen content with samples being in a metastable condition and having various states of oxygen ordering. These structural variations at the 100 Å scale are consequently suggested to cause variations in the superconducting critical temperatures below and above 90 K, which corresponds to the value of 1.8% for $\Delta a/a$ of the bulk material and, therefore, substantiates the suggestion of superconducting glassy state [5].

The metastability of the samples around 90 K as suggested by Sarikaya and Stern [5] is consistent with the prediction that there may be a spinodal decomposition region as related to oxygen ordering in the phase diagram at low temperatures predicted by Khacharuryan et al. [6] although this has not been proven yet. It has been found that careful annealing treatments can produce a bulk superconducting phase with oxygen content $0.3 < x < 0.4$ in $YBa_2Cu_3O_{7-x}$ which exhibits T_c around 60 K [7]. Furthermore, it has been observed by high-resolution transmission electron microscopy that there are isolated domains at 100 Å scale with sharp boundaries which have been attributed to regions of super- and sub-stoichiometry of O atoms about the value of seven [8]. It appears that there is a need for more quantitative analysis of structural variations in orthorhombic samples, especially in conjunction with the formations of twins which are the dominant substructural features of both single and polycrystalline samples. In this paper we

elaborate our findings on the substructural modifications in the nanoscale region with an emphasis on the twins observed in the superconducting orthorhombic phases.

It is reported that during the high-temperature (tetragonal) to low-temperature (orthorhombic) transformation of the $YBa_2Cu_3O_{7-x}$ crystal there is no measurable volume change [7,9–11]. However, transformation stresses are created because of the shape change caused by the differences in the lattice parameters of tetragonal and orthorhombic phases. The lattice parameter change is due to ordering of oxygen atoms along the [010] direction in the orthorhombic phase which causes elongation of ***b*** and contraction of ***a*** with respect to these directions in the tetragonal phase. These stresses are accommodated by the formation of transformation twins [5]. It is observed that these twins form on {110} type planes, parallel to the [001] direction of the lattice [12–14]. There can be two {110} variants [i.e. (110) and ($\bar{1}$10)] of twins in a single orthorhombic grain. Although twins are mostly uniform in a given variant, large variations frequently occur [5]. In addition, terminating twins form within orthorhombic grains [5].

In this paper we report the studies on the details of twins and their boundary shapes and structures. On the basis of our theoretical and experimental analyses we propose a mechanism for the formation and growth of twins in conjunction with tetragonal to orthorhombic transformation in $YBa_2Cu_3O_{7-x}$ compounds.

2. Spacing between twin boundaries in the orthorhombic phase

In most cases twin boundaries occur in parallel. The distance between the nearest parallel boundaries will be called the twin spacing. There are two aspects which we need to consider concerning the twin spacing, denoted as λ. The first one is an energetic and the second one is a geometrical requirement. Twins form because of the strain in the matrix that is created due to the distortion of the orthorhombic structure with respect to the tetragonal structure. The stress created is accomodated by the formation of {110} twins which results in the exchange of ***a*** and ***b*** directions in successive twinned domains as confirmed by electron diffraction studies [5].

2.1. Energy consideration

The total energy in the orthorhombic structure due to twins is given by two terms [5]. Firstly, the formation of twins costs energy E_T per twin boundary. Secondly, strains created during the tetragonal to orthorhombic transformation is accommodated by twins, hence the strain energy per unit area per twin in the domain of spacing λ is given by

$$E=\tfrac{1}{2}\Omega\lambda^2\left(\frac{\Delta a}{a}\right)^2, \tag{1}$$

where Ω is the shear modulus, and $\Delta a/a$ is the strain. Therefore, the total energy E_t per unit length in the direction of [110] becomes $E_t=(E+E_T)/\lambda$, where $1/\lambda$ is the number of twins per unit length. If E_T is independent of $\Delta a/a$, minimization of E_t with respect to λ results in

$$\lambda=\sqrt{\frac{2E_T}{\Omega}}\cdot\left(\frac{\Delta a}{a}\right)^{-1}, \tag{2}$$

which says that λ is inversely proportional to $(\Delta a/a)$; that is the higher the orthorhombicity of the lattice, the narrower the twin spacing.

It is possible to measure $\Delta a/a$ in a domain by microdiffraction technique in the transmission electron microscope. In these experiments a 100 Å diameter electron probe is formed and is placed on different twinned domains which are in [100] zone axis orientation giving 100, 010, and 110 diffraction spots in the microdiffraction patterns. Relative reciprocal distances a^* and b^* are measured directly on the diffraction patterns. As shown by Sarikaya and Stern [5], analysis of $\Delta a/a$ from many twinned regions indicate that there is no simple inverse relationship between $\Delta a/a$ and λ as given in eq. (2). This implies that the twin boundary energy E_T is also related to $\Delta a/a$. This argument is consistent with electron microscopy results [5]. Now we examine the geometrical requirement for the value of λ.

2.2. Geometrical consideration

Consider two parallel twin boundaries in an orthorhombic phase, as sketched in fig. 1 and also

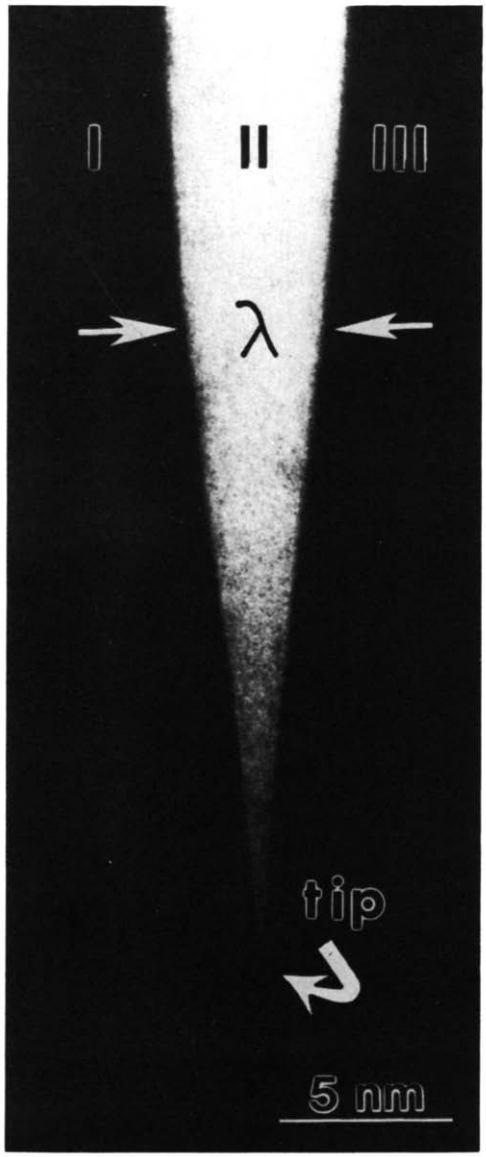

Fig. 1. TEM bright field image of two twin boundaries ending at a tip.

shown in fig. 10. When the twin boundaries I/II and II/IIII merge at a pointed tip as in fig. 1, the orthorhombic regions I and III are coherent. Under this condition, in order to have a strain-free structure, the spacing λ cannot take continuously varying values, but must be an integer multiple of the basic distance d. The latter is determined when the lengths a and b of the orthorhombic unit cell edges are given as

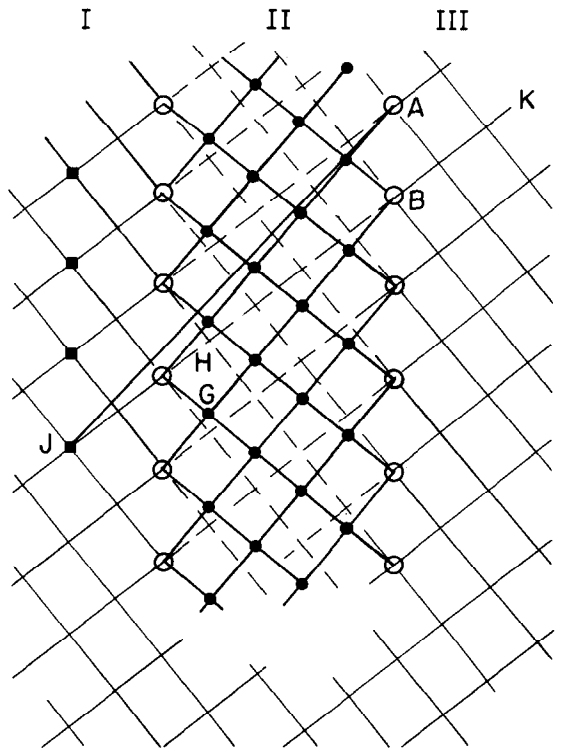

Fig. 2. Three orthorhombic domains separated by two twin boundaries (schematic).

$$d=\frac{ab}{\sqrt{2\Delta a}}, \quad \text{where} \quad \Delta a \equiv b-a>0\,. \tag{3}$$

This relation is derived as follows. The details of the geometry of the twin boundary are shown in fig. 2. Black dots are inside the II phase, open circles are on the twin boundaries. The outside orthorhombic lattices I and III are extended into the II region as broken lines. A and B are on the II/III boundary, and are nearest neighbor points. G is on the II region lattice, and H is on the hypothetical extended (broken line) lattice. G and H are on a plane parallel to the II/III boundary. When I and III are coherent, the condition that G and H can be on the I/II boundary is that the distance $\overline{GH}$ is an integer multiple of $\overline{AB}$. This condition determines the distance between the I/II and II/III boundaries and derives d in eq. (3). Analysis is a simple geometry calculation based

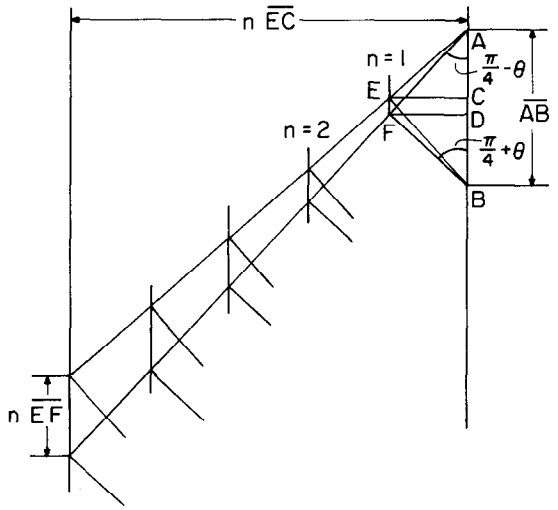

Fig. 3. Geometrical construction to determine the basic distance d in eq. (3). Note $a=\overline{AE}=\overline{BF}$ and $b=\overline{AF}=\overline{BF}$.

on fig. 3. The number of sections n which satisfies the required condition is $n\overline{EF}=\overline{AB}$. Using this n, the basic distance d in eq. (3) is derived as $d=n\overline{EC}$. It may be worth noting that when θ is defined as in fig. 3, and as in fig. 7 described below, the measure of the orthorhombicity $\Delta a/a$ is equal to 2 tan θ.

As an example, we quote one of our XRD results [13], where bulk values are $a=3.826$ Å and $b=3.891$ Å, then $a_0=3.859$ Å, $\Delta a=0.065$, and $\Delta a/a_0=0.0168$; and hence the d value is 162 Å.

The twin boundary in fig. 2 is drawn for an idealized geometry. In actual cases, within the thickness of the twin boundary, the lattice is elastically distorted, and thus the separation λ deviates from the strict integer multiple of the basic distance d. Also, the outside regions I and III in fig. 2 may be elastically disturbed near the boundary although they may be coherent away from the boundaries. Thus λ can be away from *Nd*.

The measured values of λ of many twins (>100) in electron micrographs indicate that the values vary considerably. Figure 4 gives a histogram chart of the number of twins versus the size of the measured twin spacing λ in three different regions, which may not be representative of the whole sample. Although there are some peaks (such as the ones at 100, 250, and 650 Å) the most values lie nonperiodically between the values 96 and 1460 Å. These variations in λ may

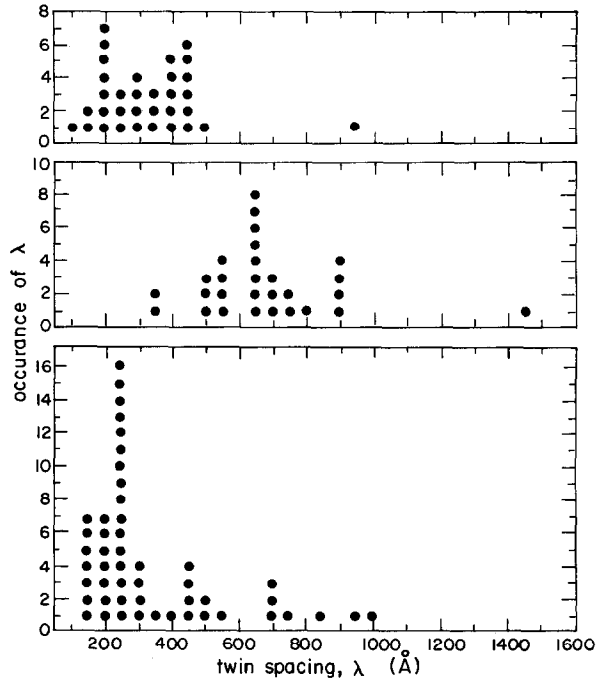

Fig. 4. Histograms showing the occurrence of various λ (twin spacings) as a function of its size in three different regions having parallel {110} twins.

be related to changes in d (stable separation) in eq. (3) or to microscopic variations in Δa away from *Nd* due to elastic strain. Since the microscopic values of a and b are not available we have shown in fig. 5 a plot of d versus x (as in $UBa_2Cu_3O_{7-x}$) that relates various bulk a and b values. The a and b values and the corresponding x values are obtained from refs. [10] and [11]. Separate curves are obtained for each set of data, although the curves converge at high values of oxygen, i.e. for $x\rightarrow 0$. The observation of variation in λ in bulk samples should not be surprising, if the variation in $\Delta a/a$, and hence in oxygen ordering in individual twins [5], are also related as in the bulk. Therefore, the basic distance d and its integer multiple λ vary across the sample for each individual twinned domain. On the same graph in fig. 5, d versus $\Delta a/a$ is also plotted as a reference showing the inverse relationship between d and $\Delta a/a$.

3. Sideway motion of a twin boundary

We interpret that the spacing λ between nearest neighboring twins adjust themselves and settles into

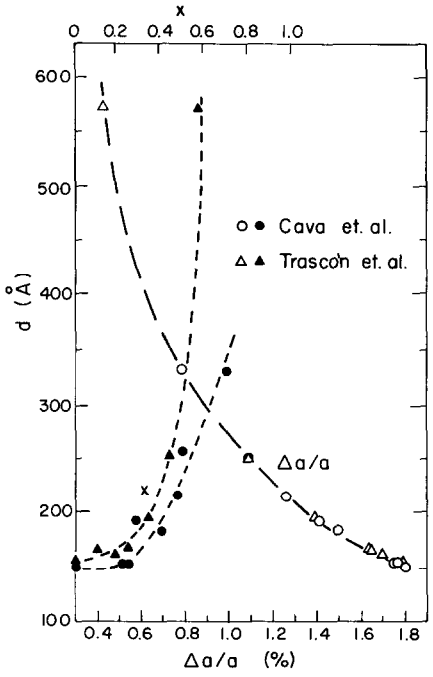

Fig. 5. Graphs showing d (basic distance) versus x (in $YBa_2Cu_3O_{y-x}$) and d versus $\Delta a/a$ (%). Data points are derived from a,b, and oxygen content given in refs. [10] (Cava et al.) and [11] (Trascon et al.).

the final configuration of stable separations dictated by $\Delta a/a$. In the process of adjustment, twin boundaries move sideways. Sideway motion needs an activation energy because the stable separations are only at or near the integer multiples of d.

Let us write a stable spacing as Nd, where d is defined in eq. (3) and N is an integer. We consider cases when the spacing λ increases from Nd. In an example shown in fig. 2, we fix the position of the I/III boundary and move the I/II boundary toward the left, for example to the position marked by squares. The lattice points in the II phase now shift; they may lie on the line AJ if the distortion is shared equally by all lattice points within the II phase Then $\Delta a/a$ decreases from the bulk phase value $(\Delta a/a)_{\text{bulk}}$. The difference of the two is the measure of the elastic stress.

The decrease of $\Delta a/a$ continues until the spacing λ reaches $(N+1)d$, at which point it bounces back to $(\Delta a/a)_{\text{bulk}}$. Based on this model, we can calculate the ratio as plotted in fig. 6. This curve is universal

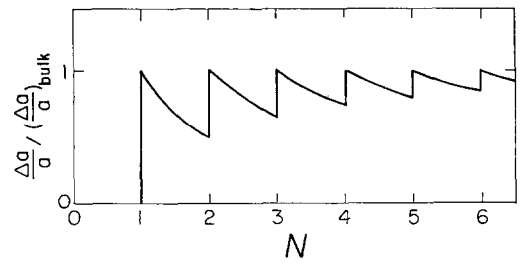

Fig. 6. Change of $\Delta a/a$ as a twin boundary moves sideways.

and is independent of the $(\Delta a/a)_{\text{bulk}}$ value. It is possible from a geometry point of view that $\Delta a/a$ increases above the bulk value, particularly when λ approaches the next stable position $(N+1)d$. However, since the tetragonal phase, for which $\Delta a/a=0$ is a metastable phase, while the phase with $\Delta a/a > (\Delta a/a)_{\text{bulk}}$ is unstable, it is more reasonable to assume that $\Delta a/a$ always stays below $(\Delta a/a)_{\text{bulk}}$. This is the nature of the model in fig. 6.

In the actual case, however, the distortion in the II phase lattice may not be shared uniformly by all lattice points, and thus the curve in fig. 6 gives only a qualitative information of the elastic stress. Evaluation of the activation energy for the sideway motion needs detailed statistical mechanical calculations.

4. Structure of the twin boundary and effective insulating thickness

Across a twin boundary the lattices on two sides are mirror images. In the orthorhombic lattice, a is slightly smaller than b because of the ordering of oxygens along the [010] direction. When the twin plane is (110) the configuration shown in fig. 7 results.

In the idealized picture, Cu atoms are located on the twin boundary, and vacancy–vacancy and oxygen–oxygen pairs are created across the interface. In a more realistic picture, the postions of Cu and oxygen atoms and vacancies will shift or redistribute on planes near the center of the interface. This redistribution may make the boundary region more tetragonal-like.

The configuration of the atomic species on and around the twin plane is different from that in the bulk. Two unit cells are outlined in fig. 7 by rectan-

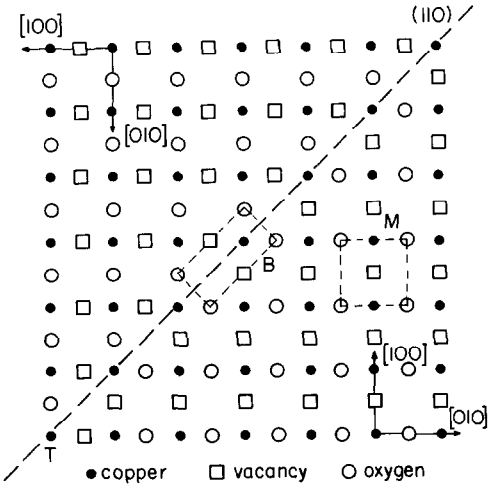

Fig. 7. The real space atomic structure on the (001) plane near a (110) twin boundary (idealized).

gles for the bulk orthorhombic region and the twin boundary region. In both cases, oxygen atoms are chosen as corners of the rectangles. In these two-dimensional configurations along [001] the point group projection symmetry of the orthorhombic unit cell is given by 2mm, and the one on the twin boundary is given by lm, which is a lower symmetry than the first. Since the boundary region has a different point group symmetry than the bulk orthorhombic region, we expect that the boundary acts as an insulating layer. The value of thickness of a boundary layer depends on the effective strain length, l_s beyond which the strain created at the twin boundary due to the atomic configuration is no longer effective, or in other words, beyond which the atomic positions are no longer shifted and the orthorhombic lattice begins. The Cu–Cu distance across the twin boundary is approximately $\sqrt{2}a_0$ $(a_0=\frac{1}{2}(a+b))$, which is the corresponding distance in the orthorhombic lattice in the [110] direction. The distance l_s of the nth layer from the boundary center is

$$l_s=\frac{n+1}{2}\frac{a_0}{\sqrt{2}}.$$

The twin widths measured in a number of electron micrographs by microdensitometer tracing give values at full-width-half-maximum between 30 and 50 Å [15]. The examination of high-resolution transmission electron microscopy images also show twin width within this range [16]. The n value at the end of this range is $n=10$. This thickness is the effective insulating layer thickness. The value of 33 Å for l_s should be compared to the measured coherence lengths (about 30 Å) mentioned in the literature [17,18]. In this overall picture, the insulating layer provided by the twin boundary surrounded by the conducting orthorhombic layers may act as Josephson junctions at the superconducting state. If that is the case, both the thickness of the twin spacing λ and the available number of twin variants in a given sample may dictate the superconducting properties. We may make a note, however, that whether a twin boundary acts as insulating or enhances superconductivity is still disputed [3,5,8,14,19]. At this stage more careful experimental data are needed to make the correlation between the substucture of the orthorhombic phase and superconducting properties.

As was commented before, the drawing in fig. 2 is an idealized case and neglects atomic distortion from lattice positions at the boundary. In actual cases, as the lattice plane KB in the III region changes into the BG direction in the II region, the change of the line direction does not occur as abruptly as drawn in fig. 2, but more gradually. When we adopt the point of view, as was mentioned in section 3, that local $\Delta a/a$ is likely to be smaller than its bulk value, it is expected that in the boundary region the local direction of the lattice line is between the KB and BG directions, as shown by M′N′ in fig. 8. In a lattice image published in ref. [16], however, the transition is not like (a) but like (b) (fig. 8), in which the direction of the BL′ portion lies outside of the line directions in II and III regions. The explanation of this structure has not been found but may be related to electron-optical alignment conditions, particularly the value of defocus in the image and the tilt of the sample with respect to the optic axis during the recording of the image.

5. Structure of the tip of twins

As we have seen in section 2, if the spacing λ between parallel boundaries is forced to deviate from an integer multiple of d in eq. (3), the lattice near the boundaries is to be distorted from the bulk struc-

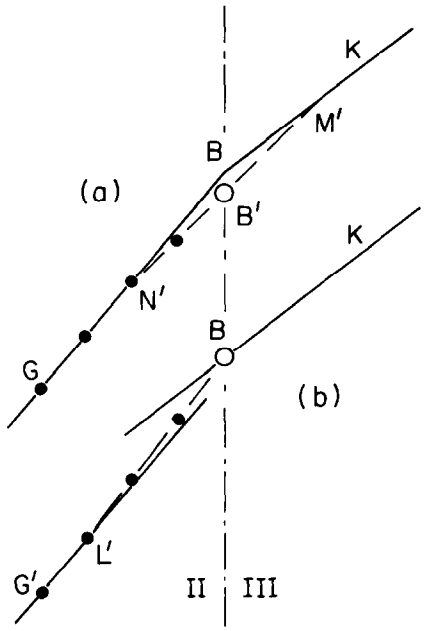

Fig. 8. Schematic illustration of lattice planes across a twin boundary.

ture. The distortion is more severe when N, in section 2.2, is smaller.

Near the tip of the merging twin boundaries as in fig. 1, the lattice distortion is very strong. As is discussed in section 2.2, out of the two possibilities of the distortion, $\Delta a/a$ being either larger or smaller than $(\Delta a/a)_{\text{bulk}}$, it is more reasonable to expect that the structure becomes closer to the tetragonal and that $\Delta a/a$ decreases toward zero. Electron microscopy studies by microdiffraction technique have indeed confirmed this hypothesis [5]. A result of a microdiffraction analysis is given in fig. 9 (reproduced using the data in ref. [5]) which displays a tip region. Here the numbers in different locations indicate the values of $\Delta a/a$ in percentages.

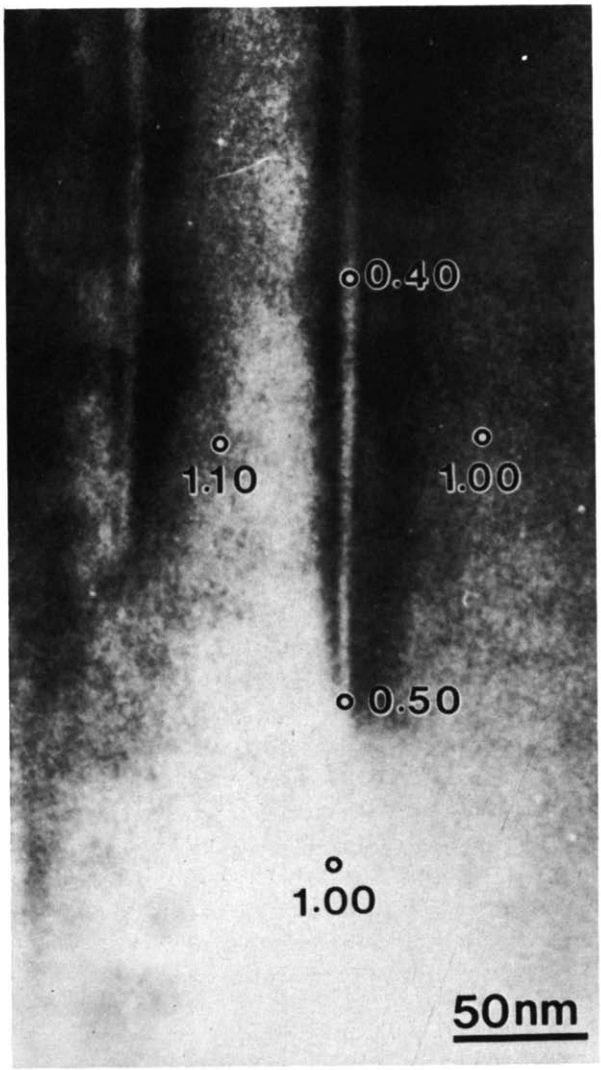

Fig. 9. Microdiffraction results of $\Delta a/a$ near a twin boundary tip (reproduction from ref. [5]).

6. Formation and growth of twins

6.1. Angle between two {110} variants of twins

As was mentioned before, two variants of twins, i.e. $(1\bar{1}0)$ and (110), exist in a single grain of the orthorhombic phase. Suh a region is displayed in fig. 10 where almost orthogonal twin boundaries in variants (A) and (B) are shown. The analysis made in fig. 3 can easily lead to the angle between two almost orthogonal twin boundaries such as in fig. 10. We perform an analysis based on fig. 11.

A twin boundary can be formed along either of the diagonal directions $\overrightarrow{AB}$ or $\overrightarrow{FP}$. The angle between the two directions deviates from $\frac{1}{2}\pi$ by 2θ, where θ is the same as that in fig. 3. Note the angle $D\hat{F}P$ in fig. 11 is equal to 2θ when FD is perpendicular to AB. For the example given in section 2.2, the angle

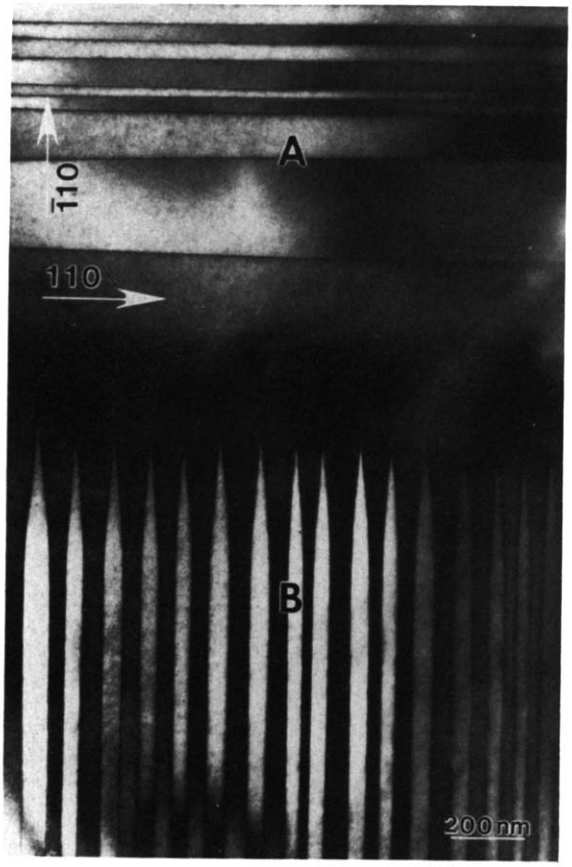

Fig. 10. Electromicrograph showing (110) and ($\bar{1}10$) variants of twins in a single grain of orthorhombic phase.

is $2\theta = 0.89°$, which is measurable. This calculated value is the same as the value 0.90 obtained from the image shown in fig. 10.

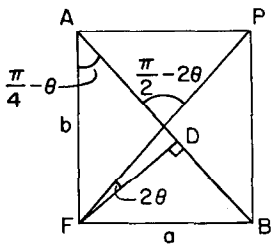

Fig. 11. Geometry of an orthorhombic unit cell.

Fig. 12. Electron micrograph of the growth stage of twins.

6.2. Formation and growth of twins

Figure 12 is believed to be the early growth stage of twins. This picture suggests the following mechanism of twin formation and growth:

(1) The twins form from the surface of a grain.

(2) Initially the spacing λ is narrow, and the twin region extends lenthwise.

(3) As the length increases, the spacing λ gradually increases through sideway motion of the boundary.

(4) Small and short twin boundary regions are seen in the picture. Probably they will be absorbed in a

longer twin boundary region as the latter moves sideways.

The image of the tip region in fig. 12 reveals that the surrounding matrix exhibit strain and suggests that twin strips, having only achieved varying and narrow spacings λ, are at a metastable equilibrium stage. This image should be compared to the one shown in fig. 10, where in the (110) variant denoted by B twins have regular spacings, and having attained the same lengths they have settled in a more stable condition. The configuration of the two variants ($\bar{1}10$) and (110) in this figure, denoted by A and B respectively, and the gradual increase of λ in A towards B may indicate that in this particular grain, the twins in A have grown first (in [110] direction) while the ones in B followed (in [$\bar{1}10$] direction). Since there is less need for strain accommodation, the twins assumed wider spacings by sideway growth at the boundary of the two variants.

Presently, the detailed mechanism of growth is not understood. Although theoretical ideas discussed in this section based on electron microscope observations on the nucleation and growth of twins seem reasonable, these hypotheses require further experimental studies.

7. Summary and conclusions

When in the future interactomic interaction potentials are obtained from quantum mechanical calculations, the equilibrium structures of both the tetragonal and orthorhombic phases are to be calculated including the values of their lattice constants. The observed lattice constants a and b in the orthorhombic phase, however, may not be the same as the theoretical equilibrium values, because of the elastic strain caused by the martensitic type tetragonal to orthorhombic transition.

The formation of twins on {110} planes in the orthorhombic phase relieves the elastic strain. In the first part of the present paper, we estimated the spacings between two parallel twin boundaries which correspond to the minimum strain condition. Such spacings are integer multiples of $d = ab/\sqrt{2}\Delta a$, where $\Delta a \equiv b - a$.

This estimate has a corollary consequence that when the inter-twin spacing λ is away from the Nd (N being an integer), $\Delta a/a$ is different from the bulk equilibrium value and hence elastic strain exists in the region between the boundaries. Because the tegragonal structure is believed to be locally stable, the deviation of $\Delta a/a$ is expected to be twoards zero (i.e., towards the tetragonal structure).

This observation further leads to the reasoning that when two twin boundaries merge and end at a tip, the region near the tip of the merging boundaries must have a value of $\Delta a/a$ smaller than the bulk value, and the local structure is closer to the tetragonal. This reasoning agrees with the observed electron microdiffraction results.

The calculation that locally stable λ is Nd suggests that when one of the parallel twin boundaries makes a parallel motion, λ becomes larger, the elastic potential energy increases, and the increment acts as the activation energy for such a parallel motion. This paper estimates the values of $\Delta a/a$ as λ increases.

There are no time series observations which show how the twin boundaries are created and how they grow. However, based on available electron micrographs we can hypothesize that twins originate at a surface of a grain, move quickly in a lengthwise motion assuming a needle shape away from the surface. The spacings, λ's, start with relatively small and uncorrelated values, and later increase as twin boundaries make sideway motion. Eventually λ's should settle at the Nd values so that elastic strain is locally minimum.

A model analysis of the (110) twin boundary reveals a different structure than the orthorhombic lattice. The width of the twin boundary is estimated to be about 30–50 Å from experimental images obtained by transmission electron microscopy. From the results discussed in this paper on the substructural variations that occur in the orthorhombic $YBa_2Cu_3O_{7-x}$ with emphasis on twins, we conclude that the samples are at metastable equilibrium and the results are consistent with samples being in the superconducting glassy state.

Acknowledgements

We are grateful to E.A. Stern for invaluable discussions. This work is sponsored by the Air Force Office of Scientific Research (AFOSR) and the De-

fense Advanced Research Projects Agency (DARPA) and monitored by AFOSR under Grant No. AFOSR-87-0114.

References

[1] K.A. Müller, M. Takashige and J.G. Bednorz, Phys. Rev. Lett. 58 (1987) 1143.
[2] K.W. Blazey, K.A. Müller, J.G. Bednorz, W. Berliner, G. Amoretti, E. Buluggiu, A. Vera and C. Matucottla, to be published.
[3] G. Deutscher and K.A. Müller, Phys. Rev. Lett. 59(15) (1987) 1745.
[4] T.R. Dinger, T.K. Worthington, W.J. Gallagher and R.L. Sandstrom, Phys. Rev. Lett. 58 (1987) 2687.
[5] M. Sarikaya and E.A. Stern, Phys. Rev. B, submitted (Jan. 8, 1988).
[6] A.G. Khachaturyan, S.B. Semenovskaya and J.W. Morris Jr., Phys. Rev. Lett., submitted (Sept. 17, 1987).
[7] I.K. Schuller, D.G. Hinks, M.A. Beno, D.W. Capone II, L. Soderholm, J.-P. Lacquet, Y. Bruynseraede, C.U. Segre and K. Zhang, Solid State Commun. 63 (1987) 385.
[8] M. Hervieu, B. Domenges, C. Michel and B. Raveau, Europhys. Lett. 4(2) (1987) 205;
B. Domenges, M. Hervieu, C. Michel and B. Raveau, ibid. (1987) 211.
[9] J.D. Jorgensen, B.W. Veal, W.K. Kwok, W.G. Grabtree, A. Umezawa, L.J. Nowicki and A.P. Paulikas, Phys. Rev. B 36 (10) (1987) 5731.
[10] R.J. Cava, B. Batlogg, C.H. Chen, E.A. Rietman, S.M. Zaharak and D. Werder, Phys. Rev. B 36(10) (1987) 5719.
[11] J.M. Trascon, L.H. Greene, B.G. Bagley, W.R. McKinnon, P. Barboux and G.W. Hall, in: Proc. Int. Workshop on Novel Mechanisms of Superconductivity, Berkeley, CA, 11–26 June 1987, eds. V. Kresin and S. Wolf (Pergamon, New York, 1987).
[12] M. Hervieu, B. Domenges, C. Michel, G. Heger, J. Provost and B. Raveau, Phys. Rev. B 36(7) (1987) 3920.
[13] M. Sarikaya, B.L. Thiel, I.A. Aksay, W.J. Weber and W.S. Frydrych, J. Mater. Sci., 2(6) (1987) 736.
[14] C.S. Pande, A.K. Singh, L. Toth, A.U. Gubser and S. Wolf, Phys. Rev. B., 36(10) (1987) 5669.
[15] B.L. Thiel and M. Sarikaya, unpublished result (University of Washington, 1988).
[16] Y. Syono, M. Kikuchi, K. Oh-ishi, K. Hirago, H. Arai, Y. Matsui, N. Kobayashi, T. Sasaoka and Y. Muto, Japan. J. Appl. Phys. 26(4) (1987) L498.
[17] For a review see J. Bardeen, In: Proc. Int. Workshop on Novel Mechanisms of Superconductivity, Berkely, CA, 1987, eds. S.A. Wolf and V.Z. Kresin (Plenum, New York, 1987).
[18] T.K. Worthington, W.J. Gallagher and T.R. Dinger, Phys. Rev. Lett. 59 (1987) 1160.
[19] C. Verea, Presented at the MRS Fall Meeting, Boston, MA, Nov. 30–Dec. 5, 1987.